bioRxiv preprint doi: https://doi.org/10.1101/340471; this version posted June 12, 2018. The copyright holder for this preprint (which was not certified by peer review) is the author/funder. All rights reserved. No reuse allowed without permission.

Five- and Six-armed Brittle Stars Make Different Currents in the Disk

Authors: Daiki Wakita[1], Yumino Hayase[2], Hitoshi Aonuma[1,3]*

Affiliations:

[1]Graduate School of Life Science, Hokkaido University, Sapporo 060-0810, Japan.

[2]Graduate School of Science, Hiroshima University, Higashi-Hiroshima 739-8526, Japan.

[3]Research Institute for Electronic Science, Hokkaido University, Sapporo 060-0812, Japan.

*Correspondence to: Hitoshi Aonuma

Research Center of Mathematics for Social Creativity, Research Institute for Electronic Science, Hokkaido University, Sapporo 060-0812, Japan.

Tel/Fax: +81-11-706-3832, Email: aon@es.hokudai.ac.jp

Abstract: Many researchers have explained how animals generate rhythmic movement. Physiological experiments and mathematical models have supported a crucial role of oscillatory neuronal activities, while robotics researches have suggested the importance of physical communication. However, it remains unclear how physical communication functions in animals. As a solution, we focused on individual difference in the number of radially symmetric arms and unique movement in brittle stars. We found that the green brittle star shrank and expanded interradii (parts of the disk partitioned by neighbor arms) with a rhythmic pattern. The movement among the interradii was unsynchronized in five-armed individuals but synchronized in a six-armed individual. To explain the relation between the pumping pattern and the body structure, we built a phenomenological model where internal fluid flows between the interradii. Based on the model, an interradius in five-armed ones makes an asymmetric flow into either neighbor, whereas that in six-armed ones makes symmetric flows into both neighbors.

Main Text:

bioRxiv preprint doi: https://doi.org/10.1101/340471; this version posted June 12, 2018. The copyright holder for this preprint (which was not certified by peer review) is the author/funder. All rights reserved. No reuse allowed without permission.

It is generally accepted that generating oscillatory patterns is crucial in virtually all animals to produce rhythmic movement. Animals utilize oscillatory neuronal activities within the central nervous systems so-called central pattern generators (CPGs) in locomotive movements (walking, swimming, flying etc.), mastication, ventilation and so on (*1-4*). However, there still remains gap between neuronal oscillation and rhythmic movement. In order to bridge the gap, many researchers built mathematical models. One of the successful models is to explain swimming pattern of lamprey, which was built based on the results of physiological experiments and simulated swimming movement (*5*). One the other hand, robotics researches suggested importance of physical communication in gait transition of animals (*6*). They demonstrated speed-dependent autonomous gait transition using a simple quadruped robot in which each limb had a CPG but there was no connection with electrical circuit between the CPGs. The brittle star-like robot designed by a similar concept was able to immediately change locomotion patterns by unexpected physical damage (*7*). Both robots coordinated limb movement by sensing local load without preprogramed patterns. However, it is still an issue how physical communication functions in animals.

Brittle stars (Ophiuroidea, Echinodermata) are marine animals characterized by radial symmetry in the body plan. The central disk has typically five arms, which partition the disk into five symmetric fan-shaped parts, called as interradii. In this study, we found that the green brittle star, *Ophiarachna incrassata* (Lamarck, 1816), moved the interradii with a rhythmic pattern after feeding (S1). This rhythmic movement reminded us of pumps, so that we call it “pumping”. Most individuals of the green brittle star have five arms with the same pumping pattern. Meanwhile, we paid attention to the fact that brittle stars sometimes have individual difference in the number of arms, namely, that of interradii. We observed pumping in a six-armed individual (S2) and recognized a different pattern in comparison to five-armed ones. Therefore, investigation into pumping of the green brittle star must provide us a right model system to understand functional role of physical communication in animals.

The green brittle star frequently showed pumping phases with an interval of 20±9 min (mean±s.d.) after feeding (Fig. 1). Individuals that were kept without feeding even for a week never showed pumping, implying the relation with digestion. Each pumping phase started with closing mouth and genital slits on the oral side of the disk. The whole contraction of the disk

bioRxiv preprint doi: https://doi.org/10.1101/340471; this version posted June 12, 2018. The copyright holder for this preprint (which was not certified by peer review) is the author/funder. All rights reserved. No reuse allowed without permission.

was immediately followed by a series of shrinkage and expansion in interradii (Fig. 2). Five-armed individuals continued a pumping phase for 57±12 sec, in which each of the five interradii repeated 3-5 cycles of movement. Based on the radius of the interradii in the aboral view, each cycle comprised a shrinking period for 5.9±1.0 sec and an expanding period for 6.5±0.8 sec at the beginning of the pumping phase (Fig. 2A). These phases gradually became longer to 7.6±1.0 and 8.1±0.9 sec respectively at the end. Meanwhile, the amplitude of the movement gradually became smaller. Each expanding period included two increasing stages in radius; the first longer one was recognized as an increase in the volume of the interradii, while the second shorter one was apparently ascribed to change in the form of the interradii. Numbered from 1 to 5 anticlockwise in the aboral view, the interradii regularly moved in the unsynchronized sequence of 1-3-5-2-4 or 1-4-2-5-3 repetitively; a cycle in one of the five interradii was followed by that in either of two distant ones with 2.2±0.5 sec delayed. The two types of sequence were observed in the same individual although a continuous pumping phase underwent either one consistently. The initially shrinking interradius was not always identical. At the end of the pumping phase, the mouth and genital slits slowly opened, so that the disk became relaxed as usual.

We then observed pumping in the six-armed individual with six symmetrical interradii by nature. Each of its pumping phases continued for 39±14 sec with the six interradii each repeating 2-4 cycles. The duration of shrinking and expanding periods at the beginning of the pumping phase was 5.4±0.8 and 6.7±0.6 sec respectively, which became 5.7±0.8 and 8.6±1.6 sec respectively at the end (Fig. 2B). Compared with the five-armed pumping pattern, the six-armed one particularly differed in terms of synchrony in movement of the interradii. Numbered from 1 to 6 likewise, the interradii moved in the synchronized sequence of 1, 3 and 5 together and then 2, 4 and 6 together repetitively; almost synchronized cycles in three distant ones followed that in the other three.

In order to explain the relation between the pumping pattern and the body structure, we built a mathematical model. Previous models explained how difference in network structure caused difference in rhythmic outputs on the basis of neuronal networks where a certain number of neurons constituted a ring (*8-10*). These models were inspired in contexts irrelevant to pumping; nevertheless, they demonstrated that the pumping-like rhythmic pattern was generated

bioRxiv preprint doi: https://doi.org/10.1101/340471; this version posted June 12, 2018. The copyright holder for this preprint (which was not certified by peer review) is the author/funder. All rights reserved. No reuse allowed without permission.

among five neurons that laterally inhibited each other. Although brittle stars possess a nerve ring in the disk (*11*), it is still unclear whether they utilize such a neuronal network there. We thus build a phenomenological model simply focusing on the physical movement of interradii, apart from neuronal interaction.

We assume that internal fluid is saved in each interradius with the volume of $u_i(t)$ individually. i takes 1 to N anticlockwise. In the shrinking period, the tension of the surface skin increases and the fluid is pushed out to another interradius. We define the pressure $p_i(t)$ at each interradius and the fluid flow from higher pressure to lower pressure.

$$\frac{du_i}{dt} = \sum_{j=1}^{N} C_{ij}\,(p_j - p_i)$$

The total volume of fluid $\sum_{i=1}^{N} u_i(t)$ is constant in time. C_{ij} is the constant indicating the connection between i-th and j-th interradii. We assume here, the connection between nearest neighbors is larger than the others.

In the expanding period, the fluid flows into the interradius. We suppose that the volume of fluid increases the pressure similarly to an elastic membrane,

$$p_i = a{u_i}^m$$

For simplicity $m = 1$. In the shrinking period, the interradius contracts to push the fluid out. We suppose a target pressure $\bar{p}$, which is much larger than that of the expanding period.

$$\tau\frac{dp_i}{dt} = \bar{p} - p_i$$

The expanding period switches to the shrinking one because of the capacity limit of $u_i(t)$. The switching occurs when $p_i(t)$ exceeds the threshold p_{th}, ($p_{th} < \bar{p}$). On the other hand, the shrinking period switches to the expanding one when no fluid is left, i.e. $u_i(t) = 0$.

At the beginning of the pumping phase, an interradius starts to shrink casually. We guess that a food may exist in one of the interradii. We take the initial condition that an interradius has a higher pressure and more fluid than the others: $(u_1, p_1) = (u_h, p_h)$ and $(u_i, p_i) = (u_0 + \xi_i, 0)$ for $i = 2, N$. Here, $u_o < u_h$, $p_h \sim \bar{p}$ and ξ_i is noise. At the end of the pumping phase, we suppose that the target pressure $\bar{p}$ becomes smaller, given the observation in which the disk becomes

bioRxiv preprint doi: https://doi.org/10.1101/340471; this version posted June 12, 2018. The copyright holder for this preprint (which was not certified by peer review) is the author/funder. All rights reserved. No reuse allowed without permission.

relaxed. With suitably chosen parameters, our numerical simulations support the experimental results well (Fig. 3).

Just changing the number of interradii from five to six, the pumping pattern changes as in the experiments (Fig. 3B). For the case of $N = 5$, the 1st interradius pushes most fluid into the 2nd and 5th ones, and then the 2nd and 5th push it into the 3rd and 4th, respectively. At the beginning, the difference between u_3 and u_4 is small. However, for example, when p_3 exceeds the threshold p_{th} and p_4 is still in the expanding period, the fluid flows from the 3rd to the 4th. The difference between u_3 and u_4 increases rapidly (around $\mathrm{t} = 1.5$ in Fig. 3), so that each interradius in five-armed individuals makes an asymmetric flow into either neighbor. The direction of the rotation depends on the initial perturbation. For the case of $N = 6$, the fluid flows started from the 1st interradius are propagated anticlockwise (1-2-3-4) and clockwise (1-6-5-4) and collide each other at the 4th one. After the collision, the 4th pushes the fluid back to the 3rd and 5th. If the 3rd has smaller volume than the 5th, the pressure of the 3rd is smaller than that of the 5th because the both are in the expanding period. More fluid flows into the 3rd than into the 5th. As a result, u_3 and u_5 come to synchronize. The 4th acts as a buffer to eliminate the difference between u_3 and u_5. This mechanism causes each interradius in six-armed individuals to make symmetric flows into both neighbors, dividing the interradii into two synchronized groups. After $t = 6$, we decrease the target pressure $\bar{p}$ gradually to zero. In the both case of $N = 5$ and 6, the period of the oscillation becomes longer and finally the oscillation vanishes in the same way as in the experiments.

References:

1. P. S. Stein, Motor systems, with specific reference to the control of locomotion. *Ann. Rev. Neurosci.* ***1***, 61-81 (1978).

2. F. Delcomyn, Neural basis of rhythmic behavior in animals. *Science* ***210***, 492-498 (1980).

3. S. Grillner, A. McClellan, C. Perret, Entrainment of the spinal pattern generators for swimming by mechano-sensitive elements in the lamprey spinal cord in vitro. *Brain Res.* ***217***, 380-386 (1981).

bioRxiv preprint doi: https://doi.org/10.1101/340471; this version posted June 12, 2018. The copyright holder for this preprint (which was not certified by peer review) is the author/funder. All rights reserved. No reuse allowed without permission.

4. E. Marder, R. L. Calabrese, Principles of rhythmic motor pattern generation. *Physiol. Rev.* ***76***, 687-717 (1996).

5. S. Grillner, Biological pattern generation: the cellular and computational logic of networks in motion. *Neuron* ***52***, 751-766 (2006).

6. D. Owaki, A. Ishiguro, A quadruped robot exhibiting spontaneous gait transitions from walking to trotting to galloping. *Sci. Rep.-UK* ***7***, 277 (2017).

7. T. Kano, E. Sato, T. Ono, H. Aonuma, Y. Matsuzaka, A. Ishiguro, A brittle star-like robot capable of immediately adapting to unexpected physical damage. *Roy. Soc. Open Sci.* ***4***, 171200 (2017).

8. U. Kling, G. Székely, Simulation of rhythmic nervous activities. *Kybernetik* ***5***, 89-103 (1968).

9. R. Suzuki, I. Katsuno, K. Matano, Dynamics of "neuron ring". *Kybernetik* ***8***, 39-45 (1971).

10. K. Matsuoka, Sustained oscillations generated by mutually inhibiting neurons with adaptation. *Biol. Cybern.* ***52***, 367-376 (1985).

11. J. L. S. Cobb, T. R. Stubbs, The giant neurone system in Ophiuroids III: the detailed connections of the circumoral nerve ring. *Cell Tissue Res.* ***226***, 675-687 (1982).

Acknowledgments: This work was partly supported by JST CREST Grant Number JPMJCR14D5, Japan.

bioRxiv preprint doi: https://doi.org/10.1101/340471; this version posted June 12, 2018. The copyright holder for this preprint (which was not certified by peer review) is the author/funder. All rights reserved. No reuse allowed without permission.

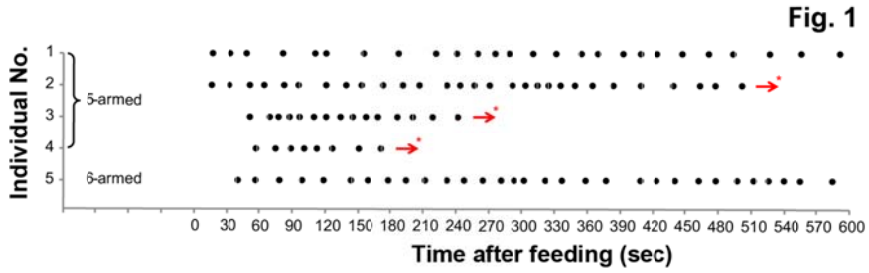

Fig. 1. Temporal frequency of pumping in the individuals of *Ophiarachna incrassata*. Each point represents a pumping phase which comprises 2-5 cycles of movement (see Fig. 2). The brittle stars show the first pumping phase 36±17 min after feeding. Then, they periodically initiate pumping for more than half days. An interval between pumping phases appears to be inconsistent (20±9 min) among individuals. Records in four five-armed individuals (No. 1-4) and a six-armed one (No. 5) are shown. Asterisks indicate no record from the arrows.

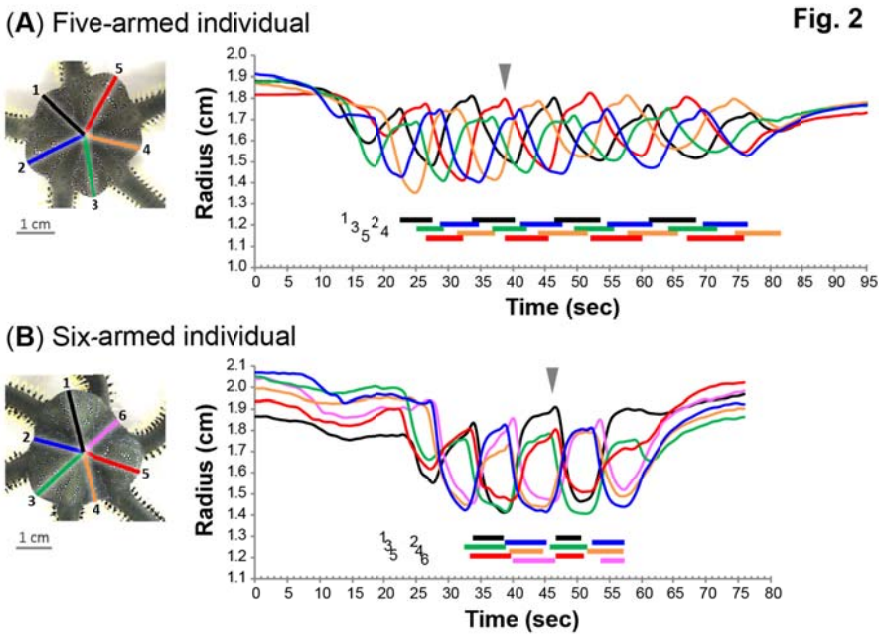

Fig. 2. Pumping of the interradii in the (**A**) five- and (**B**) six-armed individuals of *Ophiarachna incrassata*. Each snapshot shows the aboral side of the individual at the moment indicated by the arrowhead in the graph. Radius is measured from the center of the disk to the midpoint of the edge of each interradius. For each individual, the radii numbered anticlockwise are colored

bioRxiv preprint doi: https://doi.org/10.1101/340471; this version posted June 12, 2018. The copyright holder for this preprint (which was not certified by peer review) is the author/funder. All rights reserved. No reuse allowed without permission.

as in the snapshot, which corresponds to the graph in color. Colored horizontal bars under the graph represent shrinking periods of each interradius.

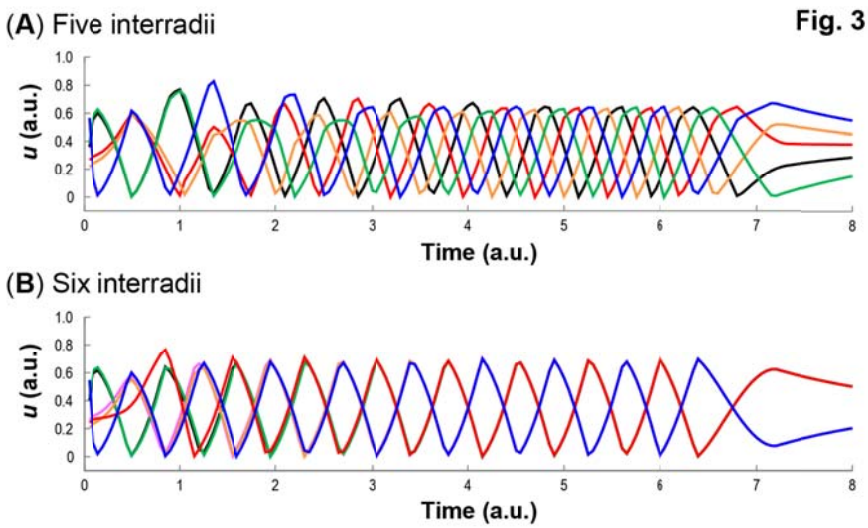

Fig. 3. Simulation of pumping on the (**A**) five and (**B**) six interradii based on a phenomenological model. u in the y-axis represents the volume of internal fluid in the interradii. Each axis is given in an arbitrary unit.

bioRxiv preprint doi: https://doi.org/10.1101/340471; this version posted June 12, 2018. The copyright holder for this preprint (which was not certified by peer review) is the author/funder. All rights reserved. No reuse allowed without permission.

Supplementary Materials:

Materials and Methods:

Intact adult individuals of the green brittle star *Ophiarachna incrassata* (Lamarck, 1816) were used in this study. They were obtained commercially and reared in laboratory aquariums (600 mm x 600 mm x 600 mm) filled with artificial seawater at 25-28°C (TetraMarin Salt Pro, Tetra Japan Co, Tokyo, Japan; salinity, 32-35‰). The disks ranged 2-5 cm in diameter and mostly had five symmetric arms. We also obtained an individual that had six symmetric arms and the disk 4 cm in diameter.

The individuals were fed with dried krill (Tetra Krill-E, Tetra Japan Co, Tokyo, Japan). Once they detect the food, their arms capture it to carry it to the mouth. After a while, their disk start rhythmic movement. The behavior of randomly selected four five-armed individuals and the six-armed one was recorded by using a time-lapse camera (TCL200, Brinno, Taipei, Taiwan). The rhythmic movement of randomly selected two five-armed ones and the six-armed one was recorded three times for each from the aboral side with a video camera (EOS8000D, Canon, Tokyo, Japan) in small acrylic cases. Successfully recorded movement was tracked using a video tracking software Kinovea (ver. 0.8.15, http://www.kinovea.org/) at 10 fps with adjustment by hand.

The numerical simulations of the mathematical model were carried out for $a = 1$, $\bar{p} = 20$, $p_{th} = 0.5$, $\tau = 1$, $C_{ij} = 0.2$ for nearest neighbors, $C_{ij} = 0.02$ for the others. For the initial condition, $u_o = 0.2$, $u_h = 1$, $p_h = \bar{p}$. After $t = 6$, the value of $\bar{p}$ is gradually reduced to zero.

Movies S1-S2

S1. Video of pumping in a five-armed individual in the aboral side.

S2. Video of pumping in a six-armed individual in the aboral side.